

Coventry
University

Coventry University Repository for the Virtual Environment (CURVE)

Author names: Ihaddoudène, A.N.T. , Saidani, M. and Chemrouk, M.

Title: Mechanical model for the analysis of steel frames with semi rigid joints.

Article & version: Post-print version

Original citation & hyperlink:

Ihaddoudène, A.N.T. , Saidani, M. and Chemrouk, M. (2009) Mechanical model for the analysis of steel frames with semi rigid joints. *Journal of Constructional Steel Research*, volume 65 (3): 631-640.

<http://dx.doi.org/10.1016/j.jcsr.2008.08.010>

Copyright © and Moral Rights are retained by the author(s) and/ or other copyright owners. A copy can be downloaded for personal non-commercial research or study, without prior permission or charge. This item cannot be reproduced or quoted extensively from without first obtaining permission in writing from the copyright holder(s). The content must not be changed in any way or sold commercially in any format or medium without the formal permission of the copyright holders.

This document is the author's final manuscript version of the journal article, incorporating any revisions agreed during the peer-review process. Some differences between the published version and this version may remain and you are advised to consult the published version if you wish to cite from it.

Available in the CURVE Research Collection: October 2012

<http://curve.coventry.ac.uk/open>

Mechanical model for the analysis of steel frames with semi rigid Joints

A.N.T.Ihaddoudène¹, M. Saidani^{2,a} and M.Chemrouk³

^{1,3} Built Environment Research Laboratory, Faculty of Civil Engineering, U.S.T.H.B.,

Algiers, Algeria

² Faculty of Engineering and Computing, Department of Built Environment, Coventry

University, Coventry, England, UK.

Abstract

The rigidity of joints is known to affect the structural behaviour of steel frames. Accurate determination of such rigidity may require use of laborious numerical modelling (such as Finite Element) of the joint. The main objective of this paper is to present a mechanical model in order to take into account the influence of the joints on the behaviour of steel frames. This mechanical model is based on the analogy of three springs, and a non deformable element of nodes describing relative displacements and rotations between the nodes and the elements of the structure. For this model, a stiffness matrix and a nodal load vector of a beam element in bending are obtained. Examples are provided to illustrate the simplicity and efficiency of the method.

Keywords: rigid; semi-rigid; connection; mechanical model; frames; plastic hinges.

^a Tel: +44 0 2476888385; fax: +44 0 2476888365. E-Mail address: m.saidani@coventry.ac.uk

Notations

$k_c; k_s$:	Secant rigidity and secant flexibility of the connection, respectively (functions of rotation Θ and moment M)
k_1, k_2 :	Elastic constants of the springs in rotation at nodes "i" and "j", respectively
$k^{(i)}$:	Flexibility in stage "i"
nl, ml :	Distance to left support and right support respectively, from gravity centre Ψ
ω :	Flexural rigidity per unit length, $\frac{EI}{l}$
Δ_i :	Relative vertical displacement between nodes "i" and "j"
V_i, M_i, V_j, M_j :	Reactions at nodes "i" and "j", in local reference.
$\overline{F_e}$:	Vector force in local reference.
Ψ :	Area of bending moment diagram for a simply supported beam.
$\Delta W^{(i)}$:	Increment of loads at stage "i"

1. Introduction

In the traditional analysis and design of steel structures, frames are analysed and designed under the simplifications that the connections behave either as pinned or rigid. The use of an ideally pinned condition implies that no moment will be transmitted from beam to column. The fully rigid condition implies that no rotation occur between the joining members (Jones et. al. [1]; Bjorhovde et. al. [2]). However, these two cases of behaviour are extreme as most connections used in common practice transmit some partial moment.

To assess the real behaviour of the frame, it is therefore necessary to incorporate the effect of connection flexibility of the frame (Bjorhovde et. al. [2]; Davison et. al. [3]; Gerstle [4]; Lui and Chen [5]; Saidani [6]). The flexibility of connections depends on the deformation of

the fasteners (bolts, end plate, angle flange cleats, etc.), the type of connections, their position and the local deformation of the assembled elements (Jaspart [7]; Jaspart and Ville de Goyet [8]; Kishi and Chen [9]).

Since the connection details consist of a member components, any change in these connection details may lead to significant variations in the connection characteristics (Yongjiu et. al. [10]; Sang-Sup and Tae-Sup [11]; Pucinotti [12]).

Some researchers such as Kishi and Chen [9], have collected available experimental results and constructed steel connection data banks that provided the user with not only the test data, but also some predictive equations. However, not every structural engineer has access to the database of experimental results. Also, when the connections detailing, beam and column sizes used in frame analysis are significantly different from the available experiments, however, the connection behaviour retrieved from a database may not, correctly, represent the actual connections.

De Lima et. al. [13] used the concept of neural networks to determine the initial stiffness of beam-to-column joints. However, the method was limited in scope and the authors did not back their results with test data to validate the method developed. Lopez et. al. [14] developed a model that takes into account the rigidity of the joints in the analysis of single-layer lattice domes. The model is based on both numerical model and test results. Del Savio et. al. [15] developed a model based on a parametric study of semi-rigid joints used for the analysis of Vierendeel girders.

Experimental results (Jones et. al. [1]; Jaspart [7]; Jaspart and Ville de Goyet [8] ; Yongjiu et al [10]; Sang-Sup and Tae-Sup [11]; Pucinotti [12]; Kishi and Chen [13]; Zoetemeijer [16]) obtained for beam-column connections show that the moment-rotation relationship is non-linear for all types of connections and varies depending on connection flexibility. It is

presented in its exponential form (Ihaddoudène [17]; Ihaddoudène and Chemrouk [18]) by the equation:

$$\Theta = kM^\alpha \quad (1)$$

Because of the high number of the parameters influencing the behaviour of connections, accurate modelling of such behaviour becomes complex. Globally, initial rigidity and the ultimate moment of the connection are the two most significant characteristics to define the behaviour of a joint (Bjorhovde et. al. [2], 1990; Ihaddoudène [17]; Ihaddoudène and Chemrouk [18]).

2. Mechanical model

The adopted model (Ihaddoudène [17]) is based on the analogy of three springs (two translational and one rotational) by considering the concept of a non-deformable element of node describing relative displacements and rotations between the nodes and the elements of the structure.

The nodes of the structure in Fig.1a are represented by a non deformable frame as in the Fig.1b where the nodes are modeled as translational and rotational springs connected to the bar element (see Fig. 1c). Thus, the ends of the bar element possess relative displacements and relative rotations.

The objective of the mechanical model is to derive in a simple way, both the stiffness matrix and the load nodal vector. For this, the bar element subjected to transversal loads (Fig. 2a) with semi-rigid joints (Fig. 2b) is considered.

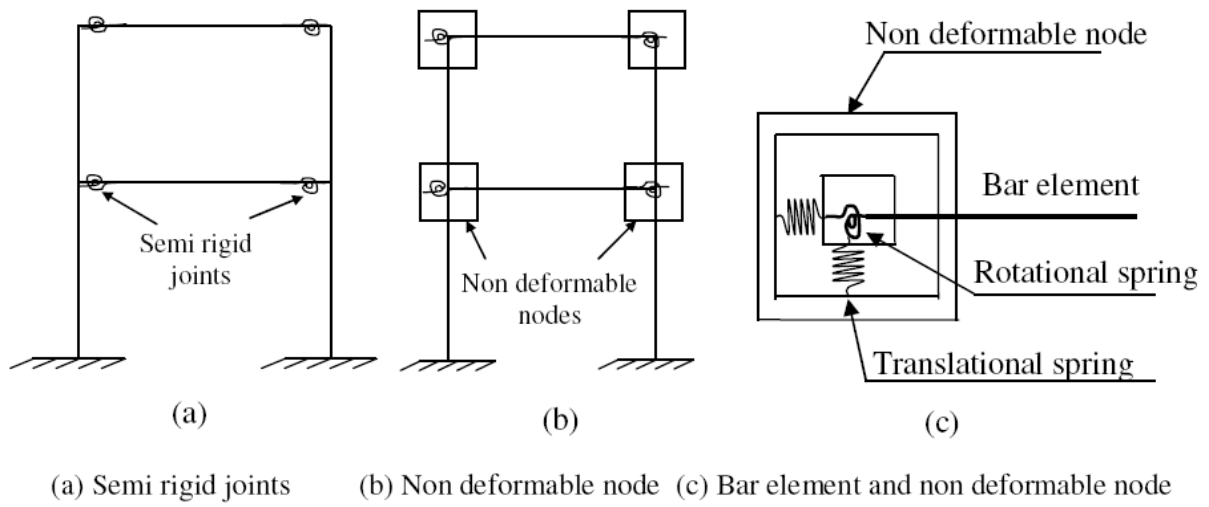
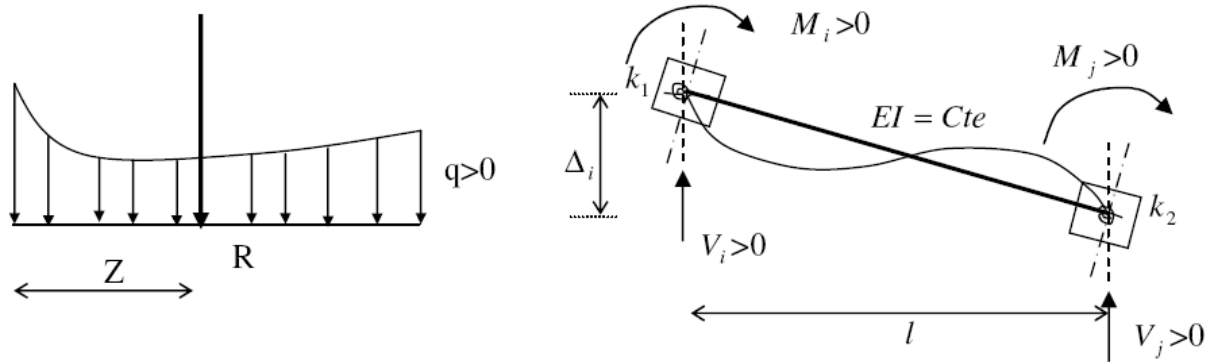
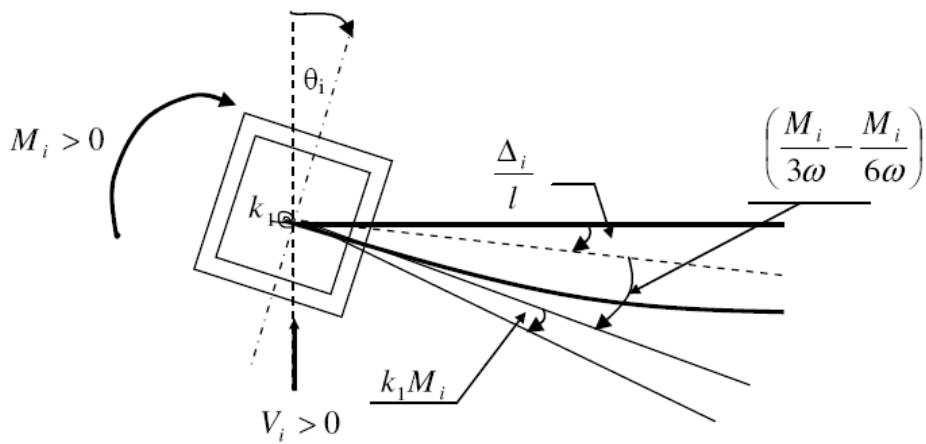


Fig.1. Mechanical model adopted



(a) Bar element under transversal loads



(b) Different rotations at node "i"

Fig.2. Non-deformable node for semi-rigid joints

2.1. Equilibrium equations and rotational deformations

The equilibrium equations may be written as:

$$V_i + V_j - R = 0 \quad (2.a)$$

$$M_i + M_j + RZ - V_j l = 0 \quad (2.b)$$

In bending, the rotational spring is the essential component and hence the equations of rotational deformations can be expressed as:

$$\Theta_i = \frac{\Delta_i}{l} + \frac{m\Psi}{\omega l} + \frac{M_i}{3\omega} + k_1 M_i^\alpha - \frac{M_j}{6\omega} \quad (3.a)$$

$$\Theta_j = \frac{\Delta_i}{l} - \frac{n\Psi}{\omega l} + \frac{M_j}{3\omega} + k_2 M_j^\alpha - \frac{M_i}{6\omega} \quad (3.b)$$

2.2. Stiffness matrix

The displacement method, which is based on stiffness matrix, is used to analyse the frame elements.

To establish the modified stiffness matrix considering the effect of connection flexibility, the direct method is used, i.e. the rigidity k_{ij} of an element "ij" is the reaction in the direction "j" due to a unit displacement in the direction "i".

The stiffness matrix, \overline{K}_e , in local coordinates is given by:

$$\overline{K}_e = \begin{bmatrix} k_{11} & k_{12} & k_{13} & k_{14} \\ k_{21} & k_{22} & k_{23} & k_{24} \\ k_{31} & k_{32} & k_{33} & k_{34} \\ k_{41} & k_{42} & k_{43} & k_{44} \end{bmatrix} \quad (4)$$

The nodes of the beam are represented by non deformable frames at each ends. As indicated by the mechanical model adopted (Ihaddoudène [17]), the beam has different flexibilities k_1 and k_2 at ends i and j respectively. In order to establish the different

elements of the stiffness matrix \overline{K}_e in local reference, equilibrium equations and rotational deformations are considered for each element, k_{ij} .

Terms k_{2j} , for instance, of the stiffness matrix are obtained by letting $\theta_i = 1$ and $\Delta_i = 0; \theta_j = 0; \Psi = R = 0$ in the Eq. (3a) and (3b).

For linear behaviour $\theta = kM^\alpha$ where $\alpha = 1$

Which gives:

$$k_{21} = -\frac{18\omega(1+2k_2\omega)}{l[4(1+3k_1\omega)(1+3k_2\omega)-1]} \quad (5.a)$$

$$k_{22} = \frac{12\omega(1+3k_2\omega)}{4(1+3k_1\omega)(1+3k_2\omega)-1} \quad (5.b)$$

$$k_{23} = -k_{21} \quad (5.c)$$

$$k_{24} = \frac{6\omega}{4(1+3k_1\omega)(1+3k_2\omega)-1} \quad (5.d)$$

The same procedure is followed in deriving all the terms of the local stiffness matrix \overline{K}_e .

For types of joints with different spring rigidities, the elements of the matrix are given in Table 1:

It is worth noting that for common steel framed buildings, in general, the connections are identical at both ends.

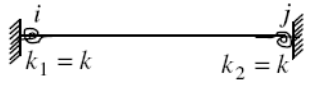
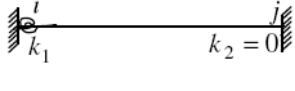
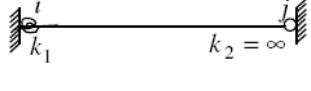
In global reference, the stiffness matrix is obtained as:

$$K_e = T_e^T \cdot \overline{K}_e \cdot T_e \quad (6)$$

In which T_e is the transformation stiffness matrix given by:

$$T_e = \left[\begin{array}{ccc|cc} \cos \beta & \sin \beta & 0 & 0 & 0 & 0 \\ -\sin \beta & \cos \beta & 0 & 0 & 0 & 0 \\ 0 & 0 & 1 & 0 & 0 & 0 \\ \hline 0 & 0 & 0 & \cos \beta & \sin \beta & 0 \\ 0 & 0 & 0 & -\sin \beta & \cos \beta & 0 \\ 0 & 0 & 0 & 0 & 0 & 1 \end{array} \right]$$

Table 1
Different configurations of the joints

k_{ij}			
k_{11}	$\frac{36\omega(1+2k\omega)}{l^2[4(1+3k\omega)^2-1]}$	$\frac{12\omega(1+k_1\omega)}{l^2(1+4k_1\omega)}$	$\frac{3\omega}{l^2(1+3k_1\omega)}$
k_{12}	$-\frac{18\omega(1+2k\omega)}{l[4(1+3k\omega)^2-1]}$	$-\frac{6\omega}{l(1+4k_1\omega)}$	$-\frac{3\omega}{l(1+3k_1\omega)}$
k_{13}	$-k_{11}$	$-k_{11}$	$-k_{11}$
k_{14}	k_{12}	$-\frac{6\omega(1+2k_1\omega)}{l(1+4k_1\omega)}$	0
k_{22}	$\frac{12\omega(1+3k\omega)}{4(1+3k\omega)^2-1}$	$\frac{4\omega}{1+4k_1\omega}$	$\frac{3\omega}{1+3k_1\omega}$
k_{23}	$-k_{12}$	$-k_{12}$	$-k_{12}$
k_{24}	$\frac{6\omega}{4(1+3k\omega)^2-1}$	$\frac{2\omega}{1+4k_1\omega}$	0
k_{33}	k_{11}	k_{11}	k_{11}
k_{34}	$-k_{14}$	$-k_{14}$	0
k_{44}	k_{22}	$\frac{4\omega(1+3k_1\omega)}{1+4k_1\omega}$	0

The angle β defines the orientation of the element with respect to the global reference system.

where $[K_e]$ is given by Eq. (7) below:

$$[K_e] = \begin{bmatrix} (N_1 + k_{11}R_1) & (N_3 - k_{11}R_3) & -k_{12}R_4 & (k_{13}R_1 - N_1) & (N_3 - k_{13}R_3) & -k_{14}R_4 \\ & (N_2 + k_{11}R_2) & k_{12}R_5 & (-N_3 - k_{13}R_3) & k_{13}R_2 & k_{14}R_5 \\ & & k_{22} & -k_{23}R_4 & k_{23}R_5 & k_{24} \\ & & & (N_1 + k_{33}R_1) & (N_3 - k_{33}R_3) & -k_{34}R_4 \\ & & & & (N_2 + k_{33}R_2) & k_{34}R_5 \\ \text{SYM.} & & & & & k_{44} \end{bmatrix} \quad (7)$$

where: $N_1 = \frac{E\Psi \cos^2 \beta}{l}$, $N_2 = \frac{E\Psi \sin^2 \beta}{l}$, $N_3 = \frac{E\Psi \sin \beta \cos \beta}{l}$, $R_1 = \sin^2 \beta$,

$R_2 = \cos^2 \beta$, $R_3 = \sin \beta \cos \beta$, $R_4 = \sin \beta$ and $R_5 = \cos \beta$.

2.3. Nodal load vector

The beam shown in Fig.3, with different flexibilities k_1 and k_2 at both fixed ends, is subjected to an external load "q". In order to establish the nodal load vector, consider different end conditions of the joints i and j .

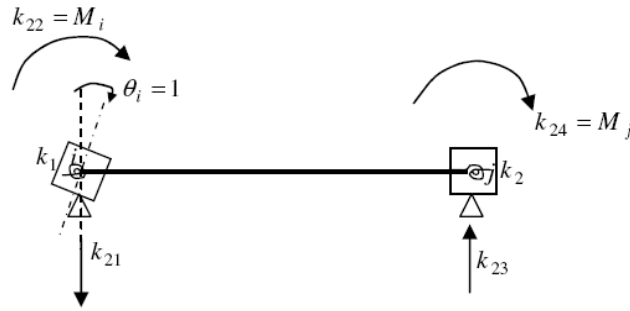


Fig.3. Element k_{2j}

The load vector in the local reference as shown in Fig. 4a is expressed as:

$$\overline{F}_e = \begin{bmatrix} \overline{X}_i \\ \overline{Y}_i \\ \overline{M}_i \\ \overline{X}_j \\ \overline{Y}_j \\ \overline{M}_j \end{bmatrix} = \begin{bmatrix} 0 \\ -V_i \\ -M_i \\ 0 \\ -V_j \\ -M_j \end{bmatrix} \quad (8)$$

where M_i , V_i , M_j and V_j for fixed ends are shown in Fig.4b and are given by :

$$M_i = -\frac{6\Psi[2m(1+3k_2\omega) - n]}{l[4(1+3k_1\omega)(1+3k_2\omega) - 1]} \quad (9.a)$$

$$M_j = \frac{6\Psi[2n(1+3k_1\omega) - m]}{l[4(1+3k_1\omega)(1+3k_2\omega) - 1]} \quad (9.b)$$

These results are derived from Eq. (2a), (2b), (3a) and (3b) of rotational deformations at nodes by setting boundary conditions $\Delta_i = \Theta_i = \Theta_j = 0$ as indicated in Fig. 4b.

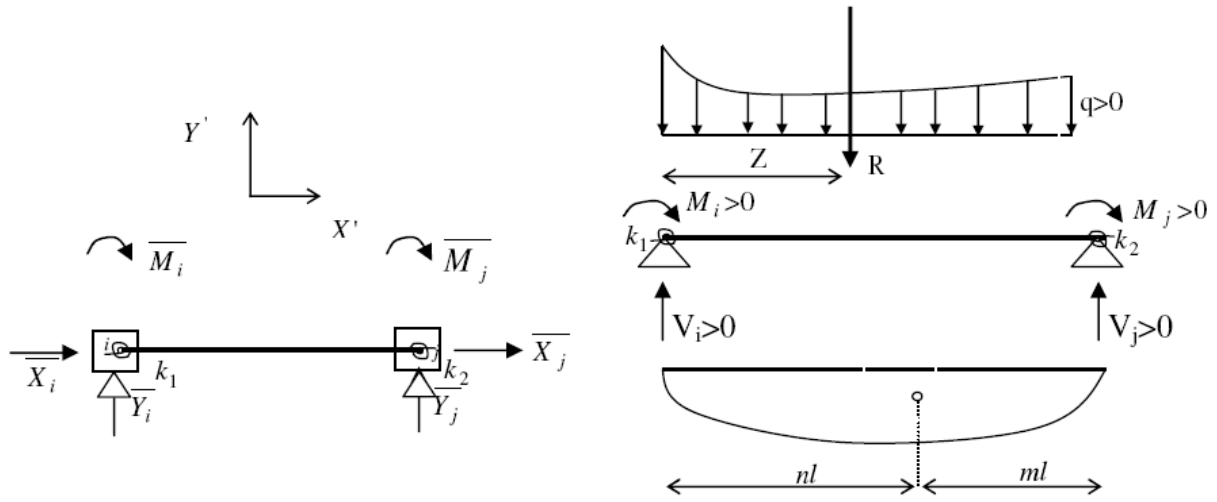


Fig.4. Bar element with semi-rigid joints

For different types of joints (with different end conditions), Table 2 summarizes the reactions M_i and M_j .

The vertical reactions V_i and V_j at nodes "i" and "j", respectively, are obtained by replacing Eq.(9.a) and (9.b) in Eq.(2.a) and (2.b) as:

$$V_j = \frac{M_i + M_j + RZ}{l} \quad (9.c)$$

$$V_i + V_j = R \quad (9.d)$$

For the case of a symmetrical frame subjected to symmetric vertical loads, half of the frame is considered. The moment reactions M_i and M_j are, hence, obtained by considering the vertical sliding support at node j (see Fig. 5), the limit conditions are now:

$$\Theta_i = \Theta_j = V_j = 0$$

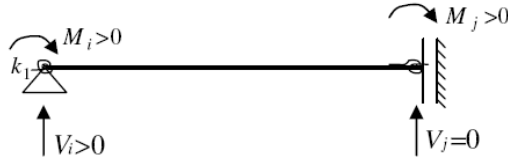


Fig.5. Propped cantilever bar element

Table 2
Reactions M_i and M_j

Different joints	Reactions	
	M_i	M_j
 $k_1 = k$ $k_2 = k$	$-\frac{6\Psi[2m(1+3k\omega) - n]}{l[4(1+3k\omega)^2 - 1]}$	$\frac{6\Psi[2n(1+3k\omega) - m]}{l[4(1+3k\omega)^2 - 1]}$
 k_1 $k_2 = 0$	$-\frac{6\Psi(2m - n)}{l[4(1+3k_1\omega) - 1]}$	$\frac{6\Psi[2n(1+3k_1\omega) - m]}{l[4(1+3k_1\omega) - 1]}$
 k_1 $k_2 = \infty$	$-\frac{3\Psi m}{l(1+3k_1\omega)}$	0
 $k_1 = 0$ $k_2 = 0$	$-\frac{2\Psi(2m - n)}{l}$	$\frac{2\Psi(2n - m)}{l}$

From Eq. (2a), (2b), (3a) and (3b) the equations become:

$$M_i = -\frac{2\Psi + RZl(1+2k_2\omega)}{2l[1+(k_1+k_2)\omega]} \quad (10.a)$$

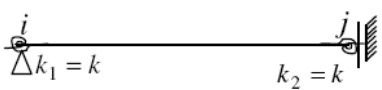
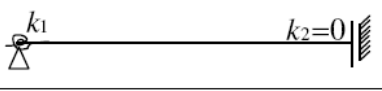
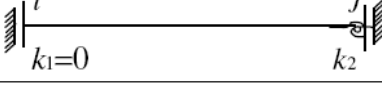
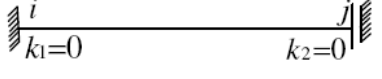
$$M_j = \frac{2\Psi - RZl(1+2k_1\omega)}{2l[1+(k_1+k_2)\omega]} \quad (10.b)$$

$$V_i = R \quad (10.c)$$

$$M_i + M_j + RZ = 0 \quad (10.d)$$

A summary of the different cases associated with the vertical sliding support is presented in Table 3 below.

Table 3
Fixed and vertical sliding ends

Support types	Reactions	
	M_i	M_j
	$-\frac{2\Psi + RZl(1 + 2k\omega)}{2l(1 + 2k\omega)}$	$\frac{2\Psi - RZl(1 + 2k\omega)}{2l(1 + 2k\omega)}$
	$-\frac{2\Psi + RZl}{2l(1 + k_1\omega)}$	$\frac{2\Psi - RZl(1 + 2k_1\omega)}{2l(1 + k_1\omega)}$
	$-\frac{2\Psi + RZl(1 + 2k_2\omega)}{2l(1 + k_2\omega)}$	$\frac{2\Psi - RZl}{2l(1 + k_2\omega)}$
	$-\frac{2\Psi + RZl}{2l}$	$\frac{2\Psi - RZl}{2l}$

In global coordinates, the vector force is obtained from:

$$F_e = T_e^T \cdot \overline{F_e} = \begin{bmatrix} V_i \sin \beta \\ -V_i \cos \beta \\ -M_i \\ V_j \sin \beta \\ -V_j \cos \beta \\ -M_j \end{bmatrix} \quad (11)$$

The internal forces are calculated by using the equation:

$$[K_e]\{U_e\} = \{F_e\} \quad (12)$$

2.4. Case study:

In order to validate the proposed model, comparisons to literature results are made. To this end, a frame of width 16m and height 6m (Chan and Chui [19]) is subjected to horizontal and vertical point loads of 10kN and 100kN, respectively as shown in Fig 6. The frame is analysed with different values of connection stiffness and for the demonstrative proposes, the semi rigid connection is related to the beam stiffness (Chan and Chui [19]).

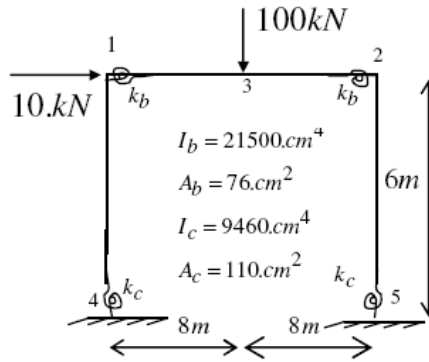
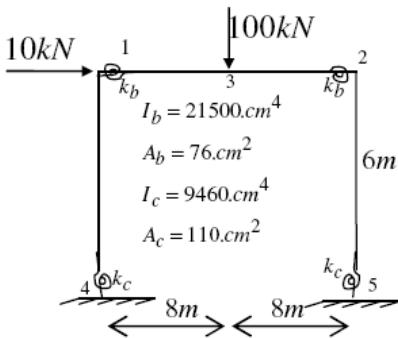


Fig.6. Portal frame (Chan and Chui [19])

From the bending moment values obtained with the present formulation and reported in the Table 4, it can be concluded that they are similar to (Chan and Chui [19]) results.

Table 4
Absolute maximum moments, this study (Chan [19])

Scheme	Rigid connection $k_b = k_c = 0$	Semi rigid connection $k_b = \frac{4EI_b}{L_b}$, $k_c = 0$	Semi rigid connections $k_b = \frac{4EI_b}{L_b}$, $k_c = \frac{EI_c}{L_c}$
 <p>Figure 6</p>	Moments	Moments	Moments
	$M_{41} = 52.2$	31.9 (31.7)	0.3392 (0.3)
	$M_{14} = 127.6$	93.7 (93.6)	80.2715 (80.3)
	$M_{52} = 87.1$	71.8 (71.5)	24.1813 (24.2)
	$M_{25} = 152.7$	113.9 (113.8)	116.4294 (116.4)
	$M_{32} = 260$	296.4 (296.3)	301.6495 (301.7)
	(kN.m)	(kN.m)	(kN.m)

3. Nonlinear analysis

The flexibility of beam to column connection is characterised by a moment-rotation curve which is nonlinear over practically the entire loading range, since the axial and shearing deformations are usually small compared to the rotational deformation.

This relationship is nonlinear for all types of connections (Yongjiu et al [10]; Sang-Sup and Tae-Sup [11]; Pucinotti [12]; Jaspert [7]; Jaspert and Ville de Goyet [8]; Kishi and Chen [9]; Zoetemeijer [16]; Cunningham [20]) and varies depending on connection flexibility. Fig. 7 shows various proposed models to fit a moment rotation curve (Cunningham [20]).

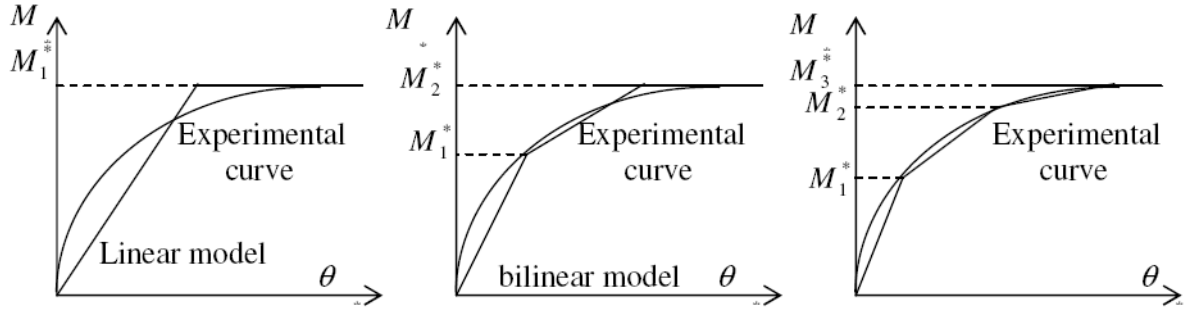


Fig.7. Various models of approximations of the moment-rotation curve

Under a monotonous loading, the nonlinear relation between the moment and rotation is expressed by:

$$M = \frac{1}{k_s} \Theta = k_c \cdot \Theta \quad (13)$$

This relation can be expressed, in each stage, by the relation:

$$M^{(j+1)} = M_{0j} + \frac{1}{k^{(j+1)}} \Theta \quad (14)$$

where : M_{0j} is the limit moment at j^{th} stage;

$$\text{For the first stage: } M^{(1)} = \frac{1}{k^{(1)}} \Theta$$

$$\text{For the second stage: } M^{(2)} = M_{01} + \frac{1}{k^{(2)}} \Theta$$

In which $M_{01} = M_1^* \left[1 - \frac{k^{(1)}}{k^{(2)}} \right]$, as indicated in Fig. 8.

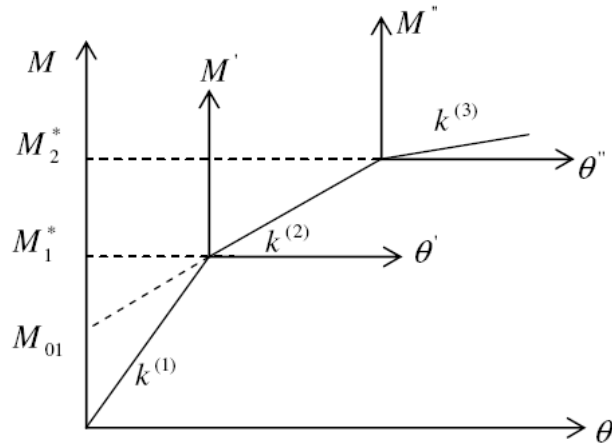


Fig. 8. Limit moments of the joint

The bilinear idealisation of the moment-rotation curve and its conservative character is justified within the framework of practical design for which the global deformation characteristics of the joints are essential. Thus, the rotational deformation represents the total response of the connection while the moment-rotation relationship defines the behaviour of the joint as a whole.

3.1. Solution process: step-by-step method

The process is divided into some steps, according to the shape of the moment-rotation curve (bilinear or tri-linear) and the state of the structure. All the joints have the same flexibility $k^{(1)}$ in the first stage of the initial portion of the moment-rotation curve. The external loads increase gradually until the load increment $\Delta W^{(1)}$ is reached permitting node “j” to reach the limit moment M_1^* as indicated in Fig.8.

The bending moment increments $\Delta M^{(1)}$ corresponding to the load increment $\Delta W^{(1)}$ are regarded as the residual moments for the second stage.

In the second stage of the curve, node "j" has a flexibility $k^{(2)}$, whereas all other nodes have flexibility $k^{(1)}$. The loads continue to increase up to value $\Delta W^{(2)}$, in such a way that the total moment reaches M_1^* , or M_2^* for node "j" as shown in Fig. 8.

The step by step process is continued until the sum of the load increments is equal to the load applied to the structure:

$$W = \sum_i^n \Delta W^{(i)} \quad (15)$$

Thus, the final moment of the structure is equal to the sum of the increments of the residual bending moments of each stage

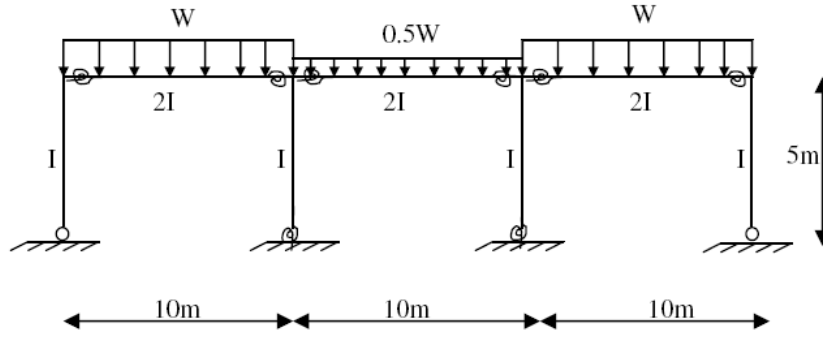
$$M = \sum_i^n \Delta M^{(i)} \quad (16)$$

3.2. Illustrative example

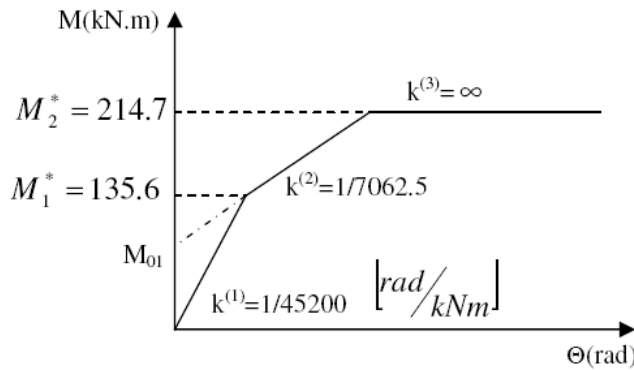
The importance of taking semi rigid connection behaviour into consideration is illustrated with the frame example below. The frame indicated in Fig.9 is used for comparing differences between the semi rigid and rigid connection assumption in terms of bending moment in beam and columns. Three behaviour cases of rigid, semi rigid linear (with $k^{(1)}$) and semi rigid bilinear behaviour ($k^{(1)}$ and $k^{(2)}$), are considered. The frame is analysed under distributed load $W = 35\text{kN/ml}$ taking the flexural rigidity per unit length as $\omega = 15067\text{kN.m}$

At the first stage, all the joints have flexibility $k^{(1)}$ and the loads increase gradually from zero until the bending moment at any joint reaches the limiting moment of this first portion:

$$M_1^* = 135.6\text{kNm} .$$



(a) Illustrative example



(b) Characteristic curve of the joint

Fig. 9. Example, adapted from [4]

The diagram of the bending moments of Fig. 10 shows that joint 2 was the first to yield reaching a value of 164.36 kNm which greater than M_1^* (135.6kNm); consequently the first increment of load is equal to $\Delta W^{(1)}$ (see Table 5). Therefore, the increments of the bending moments corresponding to this increment are summarized in the first row of Table 5.

At the second stage, joint 2 is in the second portion of the curve with the flexibility $k^{(2)}$ while the others are still in the first portion with $k^{(1)}$. The load is increased gradually from zero up to a value $\Delta W^{(2)}$ in such a way that the total moment – which is equal to the sum of the moment increments of the two stages – at a given joint reaches the limiting moment M_1^* or M_2^* for the joint “j” of the second portion of the curve.

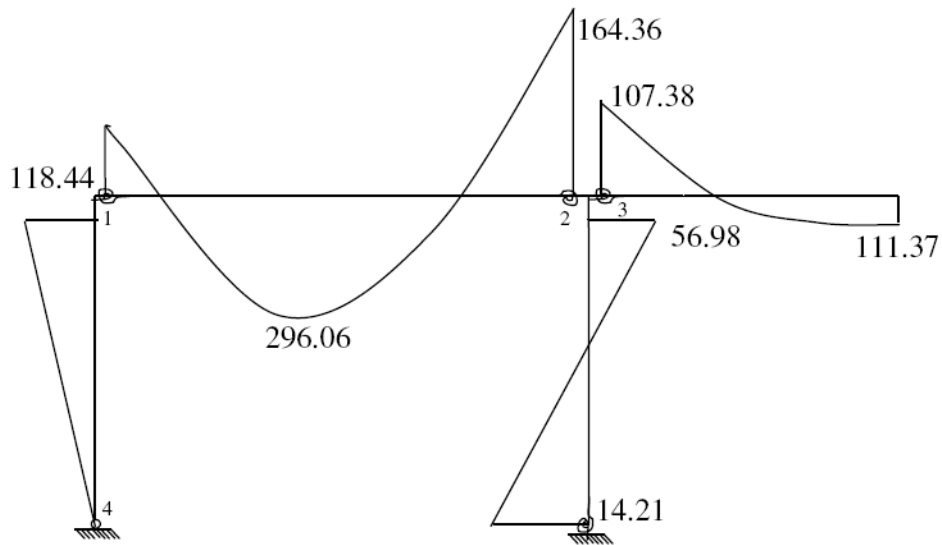


Fig. 10. Bending moment diagram (first stage)

Table 5
Values of moment increments

i^{th} Stage	$\Delta W^{(i)}$	$\Delta M_1^{(i)}$	$\Delta M_2^{(i)}$	$\Delta M_3^{(i)}$	$\Delta M_4^{(i)}$	$\Delta M_5^{(i)}$	$\Delta M_6^{(i)}$	$\Delta M_7^{(i)}$
1	28.875	-97.71	-135.6	-88.59	11.82	91.88	-46.9	244.25
2	6.124	-23.97	-9.25	-13.74	-1.22	24.53	4.48	59.94
Σ	35.00	-121.68	-144.85	-102.33	10.60	116.41	-42.42	304.19
Units	kN			$kN.m$				

In this case, the remaining external load is lower than $\Delta W^{(2)}$. The bending moment increments at the critical sections of the frame corresponding to this remainder of load ΔW are given in Table 5; the final bending moment of the frame is equal to the sum of the increments of the two stages: $M_j = \sum_1^2 \Delta M_j^{(2)}$.

The results obtained in Table 5 comply with the previous assumption and constitute a solution to the problem. To show how the discrepancy between the rigid and semi rigid joint

cases is significant, the same frame is considered with different joints behaviour. The bending moment diagrams of Fig.11 show that the difference between a rigid and a semi rigid frame is significant and is approximately 30%. It can be concluded that the connections influence greatly the behaviour of the frame.

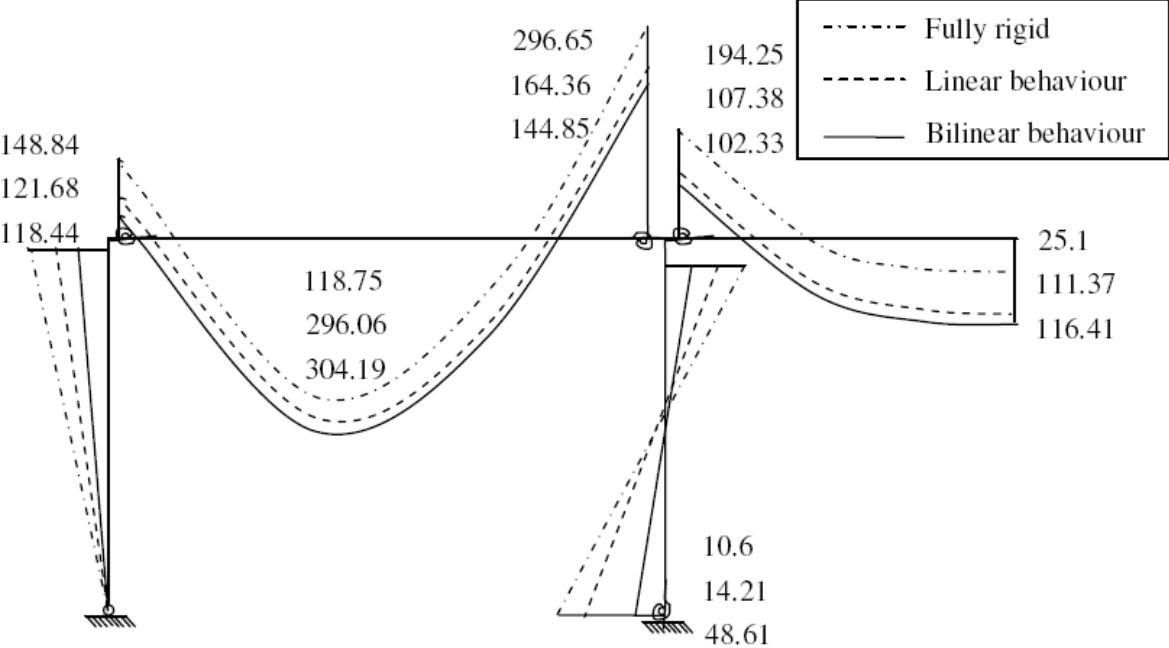


Fig. 11. Bending moment diagrams using different models.

4. Plastic analysis

The frame behaviour is deteriorated by successive formation of plastic hinges. Since the frame equilibrium path is non linear, the analysis has to be performed step-by-step, increasing the load incrementally.

When adopting the plastic hinge concept, both the joint and the section members can be represented by the non linear elasto-plastic moment-rotation curve with different flexibility $k^{(i)}$ for the joints, as shown in the Fig.12a and 12b, respectively.

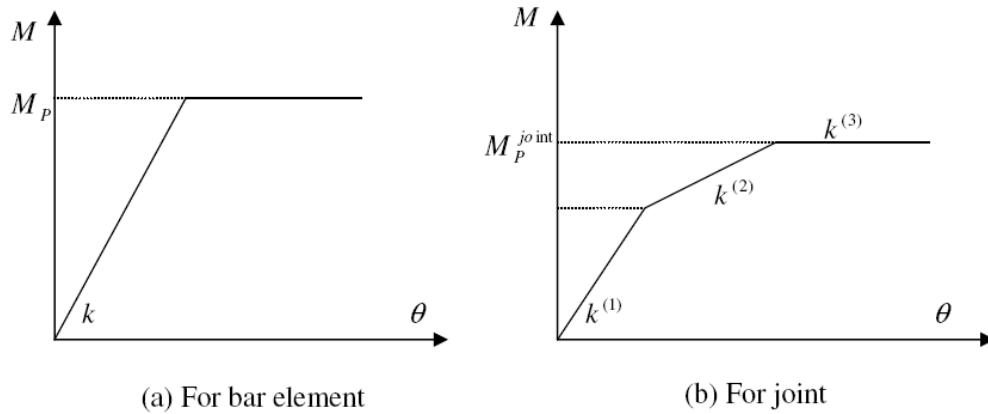


Fig. 12. Characteristic curves used in modeling

It is assumed that frame members and joints can be loaded up to their plastic moment M_p and M_p^{joint} respectively.

In this method, the behaviour and the state of the structure at any stage of the loading are followed step-by-step.

The calculations are carried out as a succession of linear steps and the loading is carried out gradually until the failure of the structure is reached. The final value of the plastic load is the sum of the load increments: $W_p = \sum \Delta W^{(i)}$

It is assumed that the behaviour of the structure between two successive stages of calculations is linear and that the state of the internal forces within each stage can be determined by the finite element method with the displacement model.

To illustrate the solution procedure of the method, a one-bay, one-story portal frame of Fig.13 is considered. In this example, the moment rotation of the joints and frame elements are assumed to be elasto-plastic. An IPE 330 steel profile was used on the beam and columns.

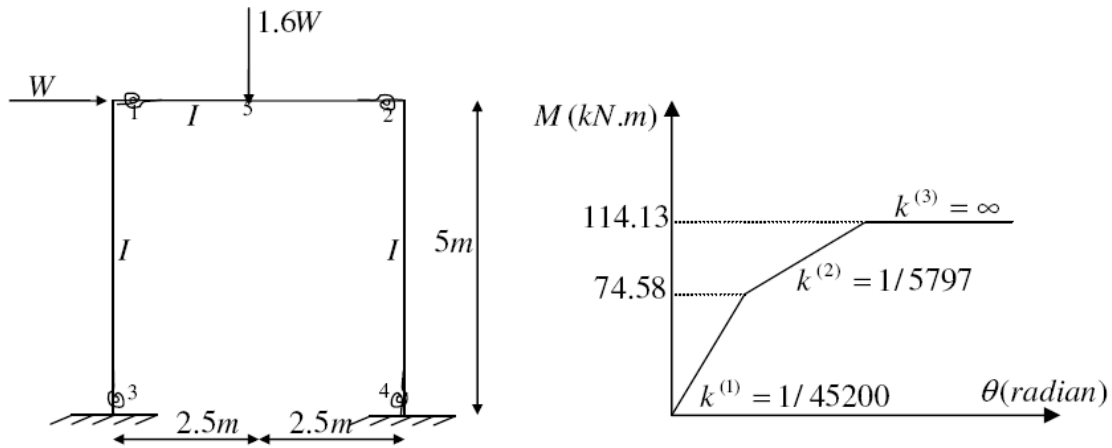


Fig. 13. Frame with semi rigid joints

The plastic moments of the joint and a frame element are:

$$M_p^{joint} = 114.13 kNm \text{ and } M_p = 2S_x \sigma_e = 192.96 kNm, \text{ respectively.}$$

The formulation of the problem in this case can be extracted from the formulation of previous sections.

At the first stage, all the joints have the same flexibility $k^{(1)}$ as is shown in the first row of Table 6 and Fig.14. Since the value of the moment $\Delta M_2^{(i)} = -74.58 kNm$ (First row of Table 8), joint 2 reaches the limit moment of the first portion and then has the flexibility $k^{(2)}$ as indicated in the second row of Table 6.

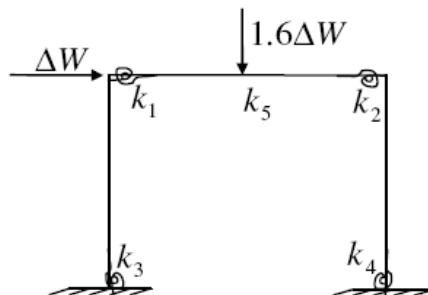
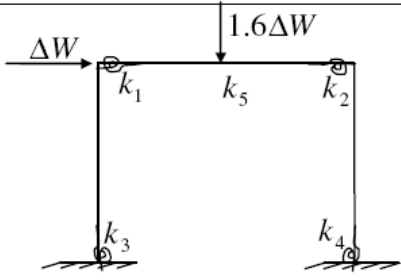


Fig. 14. Illustrative example

As the load is increased, a first plastic hinge forms at joint 2 (fifth row, Table 6) the result of this load increment is reported in the fifth row of Table 8.

In the next stage, for the rest of loading, plastic hinge will form one by one. As can be seen in Fig.15, a certain sequence of plastic hinge is found.

Table 6
Calculation process

Scheme	I^{th} Stage	Flexibility k in the critical sections				
		k_1	k_2	k_3	k_4	k_5
 <p>Figure 14</p>	1	$k^{(1)}$	$k^{(1)}$	$k^{(1)}$	$k^{(1)}$	0
	2	$k^{(1)}$	$k^{(2)}$	$k^{(1)}$	$k^{(1)}$	0
	3	$k^{(1)}$	$k^{(2)}$	$k^{(1)}$	$k^{(2)}$	0
	4	$k^{(1)}$	$k^{(2)}$	$k^{(2)}$	$k^{(2)}$	0
	5	$k^{(1)}$	$k^{(3)}$	$k^{(2)}$	$k^{(2)}$	0
	6	$k^{(1)}$	$k^{(3)}$	$k^{(2)}$	$k^{(3)}$	0
	7	$k^{(2)}$	$k^{(3)}$	$k^{(2)}$	$k^{(3)}$	0
	8	$k^{(2)}$	$k^{(3)}$	$k^{(3)}$	$k^{(3)}$	0

The bending moments in the critical sections due to the unit load for all the stages of load increments are reported in Tables 7 and 8.

Table 7
Bending moments at critical sections at each stage of unit load increments

I^{th} Stage	$\Delta \bar{W}^{(i)}$	$\Delta \bar{M}_1^{(i)}$	$\Delta \bar{M}_2^{(i)}$	$\Delta \bar{M}_3^{(i)}$	$\Delta \bar{M}_4^{(i)}$	$\Delta \bar{M}_5^{(i)}$	$\Delta u_2^{(i)} \omega$
1	1.0	0.5314	-1.6678	-1.1864	1.6142	1.4317	2.18351
2	1.0	0.6835	-0.9865	-1.6080	1.7221	1.8485	2.99000
3	1.0	1.0320	-1.0380	-2.1329	0.7980	2.0030	3.86140
4	1.0	1.3550	-1.3507	-1.1476	1.1469	2.0021	5.67572
5	1.0	1.8970	0.0	-1.9620	1.4216	2.9485	8.45210
6	1.0	2.7272	0.0	-2.2720	0.0	3.3645	11.1971
7	1.0	2.0605	0.0	-2.9379	0.0	3.0302	15.7052
8	1.0	5.0000	0.0	0.0	0.0	4.5000	19.1666
Units	kN			kNm			kNm ²

The value of the plastic failure load which corresponds to the total of the load increments at all stages and the horizontal displacement at the top of the columns just prior to the plastic failure are respectively $W_p = 91.293kN$ and $u_2 = 9.57cm$ as indicated in the Table 8.

Table 8
Bending moments at the critical sections corresponding to load increment $\Delta W^{(i)}$

$I^{th} Stage$	$\Delta W_1^{(i)}$	$\Delta M_1^{(i)}$	$\Delta M_2^{(i)}$	$\Delta M_3^{(i)}$	$\Delta M_4^{(i)}$	$\Delta M_5^{(i)}$	$\Delta u_2^{(i)}$
1	44.716	23.762	-74.58	-53.050	72.181	64.020	0.0197
2	1.393	0.952	-1.375	-2.240	2.399	2.575	0.0008
3	9.044	9.333	-9.388	-19.290	7.208	18.115	0.0071
4	21.313	28.879	-28.787	-24.458	24.443	46.670	0.0245
5	5.556	10.540	0.0	-9.401	8.999	16.383	0.0095
6	0.408	1.114	0.0	-0.928	0.0	1.373	0.0009
7	1.621	3.340	0.0	-4.763	0.0	4.912	0.0051
8	7.242	36.210	0.0	0.0	0.0	32.589	0.0281
Σ	91.293	114.13	-114.13	-114.13	114.13	182.637	0.0957
Solution	91.304	114.13	-114.13	-114.13	114.13	182.608	
Units	KN		KN.m				m

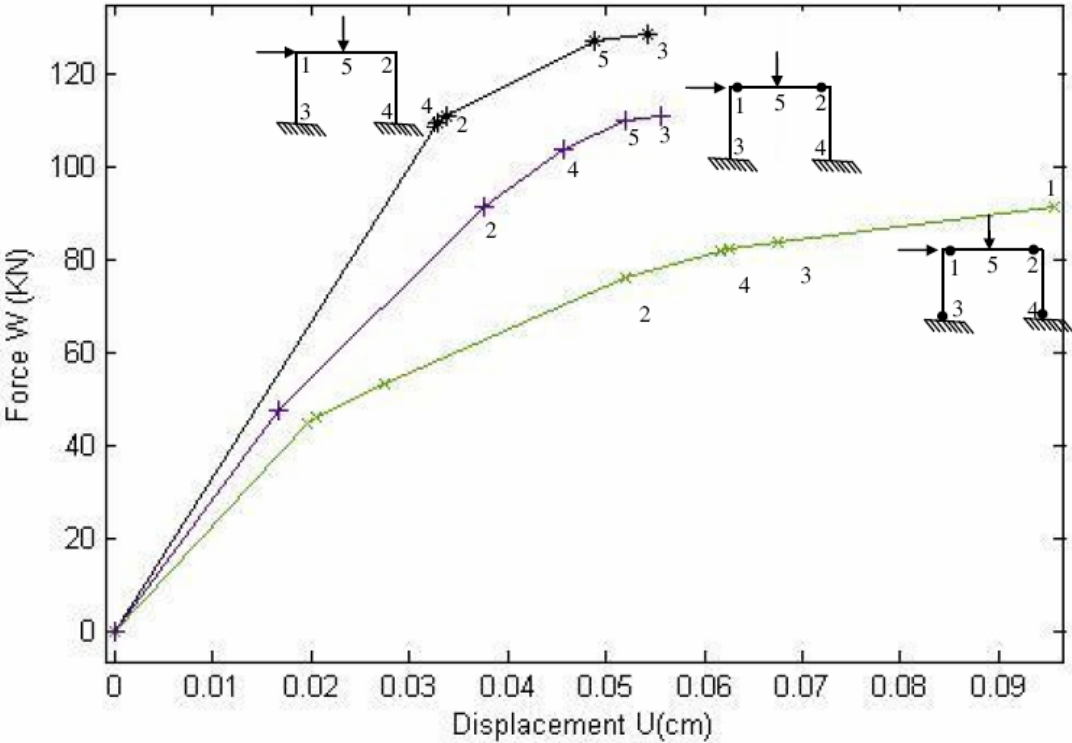


Fig. 15. Order of appearance of the plastic hinges for different types of joints

To evaluate the influence of the semi-rigid joints on the distribution of the bending moments and on the order of appearance of the plastic hinges in the structure, the previous frame is examined with different joint connections.

The relation between the load and horizontal displacement with each stage of behaviour, as well as the order of appearance of the plastic hinges within the frame for various joints are given in Fig. 15.

In order to justify the method and the formulas developed from the mechanical model proposed, one can utilize the plastic method based on static and kinematic theorems which solutions give upper and lower bounds, respectively, of the true solution (see Table 9).

Table 9
Comparaisons (Ihaddoudène [17])

Scheme			
Load failure	91.293 kN	111.122 kN	128.64 kN
Verification	91.304 kN	111.122 kN	128.64 kN
Horizontal displacement	0.0957 m	0.0556 m	0.0542 m

It can be seen that under the same applied loads, the horizontal displacements of the semi-rigid frame are larger than those of the frame with rigid joints.

The real behaviour of the joints changed the sequence of plastic hinges formation and precipitated plastic failure. In these cases, the mechanism of collapse has changed and the load capacity of the structure was reduced.

Finally, collapse of the structure occurs for lower loads compared to the usual case used for structural analysis.

5. Conclusions

The influence of the flexibility of connections in steel frames is investigated and a simple method of analysis and design is provided through a mechanical model for the joints. For a more accurate analysis of a structure the real behavior of the joints should be taken into consideration.

The numerical examples presented showed the need for taking into account the flexibility of the joints, shown to affect both internal forces distribution and elements deformation.

The flexibility affects not only the force distribution in beams and columns of the frame but also the order of appearance of the plastic hinges in the frame and the failure load in the structure as well.

The method developed in this study offers a simple direct and versatile approach to the structural analysis with semi-rigid joints compared to the complex models and cumbersome nonlinear procedures in use.

References

- [1] Jones, S.W., Kirby, P.A. and Nethercot, D.A. The analysis of frames with semi-rigid connections: A state of the art report, *Journal of Constructional Steel Research*, 1983, **3**(2), 2-13.

- [2] Bjorhovde, R., Colson, A. and Brozzetti, J. Classification system for beam-to column connections, *J. Str. Eng.* 1990, **116**(11), 3059-3077.

- [3] Davison, J.B., Kirby, P.A. and Nethercot, D.A. Rotational stiffness characteristics of steel beam-to-column connections, *Journal of Constructional Steel Research*, 1987, **8**, 17-54.
- [4] Gerstle, K.H. Effect of connections on frames, *Journal of Constructional Steel Research*, 1988, **10**, 241-267.
- [5] Lui, E.M. and Chen, W.F. Steel frame analysis with flexible joints, *Journal of Constructional Steel Research*, 1987, **8**, 161-202.
- [6] Saidani, M. The effect of eccentricity connection on the distribution of axial force and bending moments in RHS lattice girders. *Journal of Constructional Steel Research*, 1998, Vol.47, No.3, pp.211-221.
- [7] Jaspert, J.P. Etude de la semi-rigidité des nœuds poutre-colonne et son influence sur la résistance et la stabilité des ossatures en acier, Ph.D. Thesis, University of Liège, Belgium, 1991.
- [8] Jaspert, J.P. and Ville de Goyet, V. Etude expérimentale et numérique du comportement des structures composées de poutres à assemblages semi-rigides, *Construction Métallique*, 1988, **2**, 31-49.
- [9] Kishi, N. and Chen, W.F. Semi-rigid steel beam to column connections: Data base and modeling, *J. Str. Eng.*, 1989, **115**(1), 105-119.

[10] Yongjiu, S., Gang, S. and Yuanqing, W. Experimental and theoretical analysis of the moment-rotation behaviour of stiffened extended end-plate connections, *Journal of Constructional Steel Research*, 2007, **63**, 1279-1293.

[11] Sang-Sup, L. and Tae-Sup, M. Moment-rotation model of semi rigid connections with angles, *Engineering Structures*, 2002, **24**, 227-237.

[12] Pucinotti, R. Top-and-seat and web angle connections: prediction via mechanical model, *Journal of Constructional Steel Research*, 2001, **57**, 661-694.

[13] De Lima, L.R.O., Vellasco, P.C.G., De Andrade, S.A.L., Da Silva, J.G.S. and Vellasco, N.M.B.R. Neural networks assessment of beam-to-column joints. *Journal of the Brazilian Society of Mechanical Sciences and Engineering*. 2005, Vol.27 no.3, Rio de Janeiro, pp.314-324,

[14] Lopez, A., Puente, I. and Serna, M.A. Numerical model and experimental tests on single-layer latticed domes with semi-rigid joints. *Computers and Structures*. 2007, Volume 85, Issues 7-8, pp. 360-374.

[15] Del Savio, A.A., Martha, L.F. and De Andrade, S.A.L. Structural modelling of Vierendeel beams with semi-rigid joints. *Proceedings of the XXVI Iberian Latin-American Congress on Computational Methods in Engineering – CILAMCE 2005*, Brazilian Assoc. for Comp. Mechanics (ABMEC) & Latin American Assoc. of Comp. Methods in Engineering (AMC), Guarapari, Espírito Santo, Brazil, 2005.

- [16] Zoetemeijer, P. Summary of the research on bolted beam-to-column connections, Stevin Laboratory Report 25-6-90, Delft University of Technology, Delft, The Netherlands; 1990.
- [17] Ihaddoudène, A.N.T. Analyse non-linéaire des structures métalliques à assemblages semi-rigides”, Masters Thesis, Civil Engineering Institut, USTHB, Algeria ; 1995.
- [18] Ihaddoudène, A.N.T. and Chemrouk, M. Influence of Semi-Rigid Joints on the Behaviour of Steel Beam-Column Structures, *Proceedings of the International Conference on Computational & Experimental Engineering & Science*, Madeira, Portugal, July. 2004.
- [19] Chan, S.L. and Chui, P.P.T. Non-linear static and cyclic analysis of steel frames with semi rigid connections, 2000, Elsevier Science Ltd, 336p.
- [20] Cunningham, R. Some aspects of semi-rigid connections in structural steelwork, *The Structural Engineer*, 1990, **68**(5), 85-92.